An investigation of the optimal load paths for the hydroforming of T-shaped tubes

M. Kadkhodayan & A. Erfani-Moghadam

The International Journal of Advanced Manufacturing Technology

ISSN 0268-3768
Volume 61
Combined 1-4

Int J Adv Manuf Technol (2012) 61:73-85
DOI 10.1007/s00170-011-3700-0

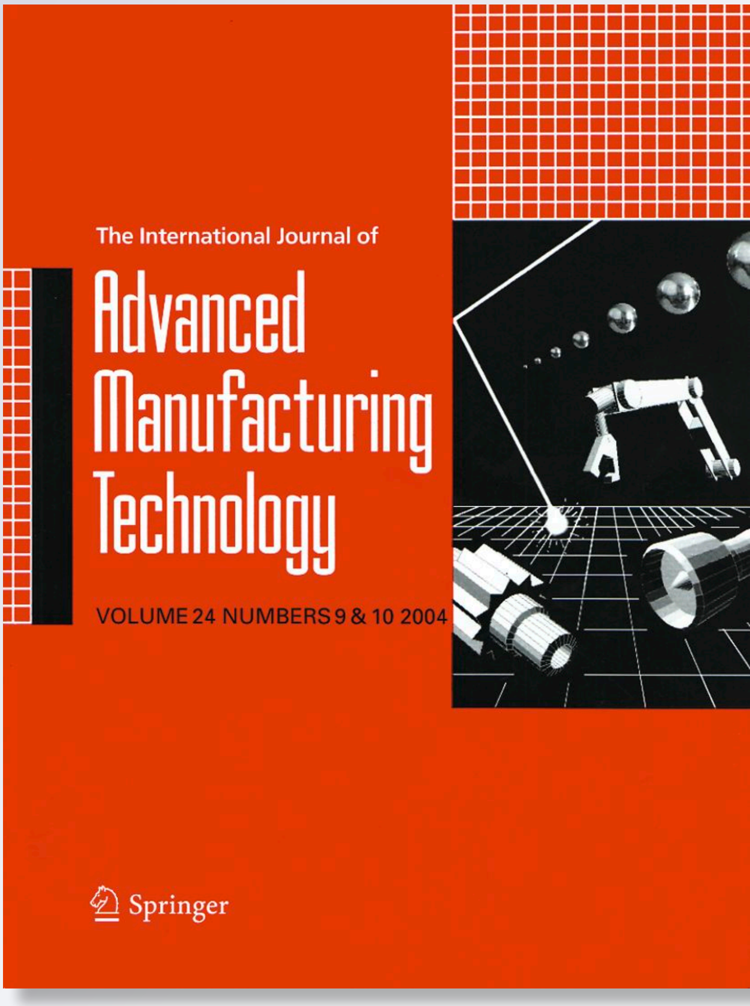

Springer

Int J Adv Manuf Technol (2012) 61:73–85
DOI 10.1007/s00170-011-3700-0

ORIGINAL ARTICLE

An investigation of the optimal load paths for the hydroforming of T-shaped tubes

M. Kadkhodayan · A. Erfani-Moghadam

Received: 21 February 2011 / Accepted: 10 October 2011 / Published online: 26 October 2011

Abstract This paper proposes a new method to design the optimal load curves for hydroforming T-shaped tubular parts. In order to assess the mathematical models, a combination of design of experiment and finite element simulation was used. The optimum set of loading variables was obtained by embedding the mathematical models for tube formability indicators into a simulated annealing algorithm. The adequacy of the optimum results was evaluated by genetic algorithm. Using this method, the effect of all loading paths was considered in hydroforming of T-shaped tubes. Eliminating of variables with lower effect could simplify the problem and help designers to study the effect of other parameters such as geometrical conditions and loading parameters. Applying the optimal load paths obtained with the proposed method caused an improvement in the thickness distribution in the part as well as a decrease in maximum pressure.

Keywords Hydroforming · Load paths · Design of experiment · Optimization

1 Introduction

To reduce air pollution and fuel consumption to satisfy the demands for increased safety in vehicle body structures that are also lightweight and cost effective, new manufacturing processes are required. Using hollow parts instead of solid bars can reduce the weight of a body while improving its strength; therefore, the hydroforming of thin-walled structures and hollow shapes is attractive for manufacturing. The major advantages of tubular hydroforming include weight reduction of the component, superior structural strength, and stiffness [1]. Manufacturing a high-quality product depends on various factors, such as loading curves, material formability, and lubrication conditions. Generally, there are three functions of time loading paths in this process including internal pressure, axial feeding, and counterpunch displacement. The application of proper loading parameters in this process plays a significant role on the formability to prevent the typical defects, such as wrinkling, thinning, or bursting. The process of adjusting the loading conditions in tube hydroforming is also known as the design of load paths and many researchers have focused on improving product manufacturing by optimizing the loading curves. Rimkus et al. [2] presented the principles involved in the design of load-curves for the simulation and production of a component with hydroforming. They used typical load curves for internal pressure that were represented by three different phases, consisting of filling the tube (until the yielding of the tube), expanding the tube, and calibration. Imaninejad et al. [3] used finite element simulation and optimization software to optimize the loading paths for closed-die T-branch tube hydroforming. Koç and Altan [4] used two-dimensional finite element analysis (FEA) to generate simple design rules on geometrical and process parameters. Lang et al. [5] investigated how to control the shape of the wrinkle waves and its effect on thickness

M. Kadkhodayan (✉) · A. Erfani-Moghadam
Department of Mechanical Engineering,
Ferdowsi University of Mashhad,
Mashhad, Iran
e-mail: kadkhoda@um.ac.ir

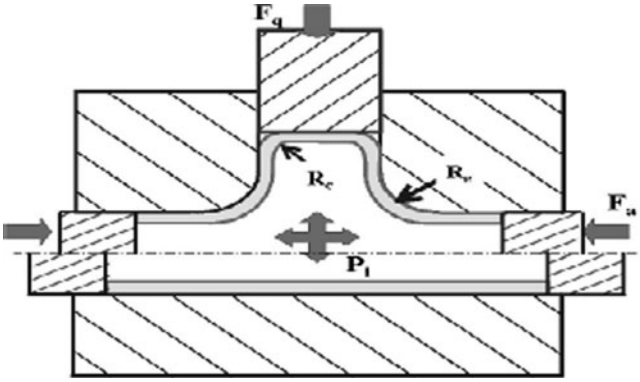

Fig. 1 Schematic of T-shaped tube hydroforming [19]

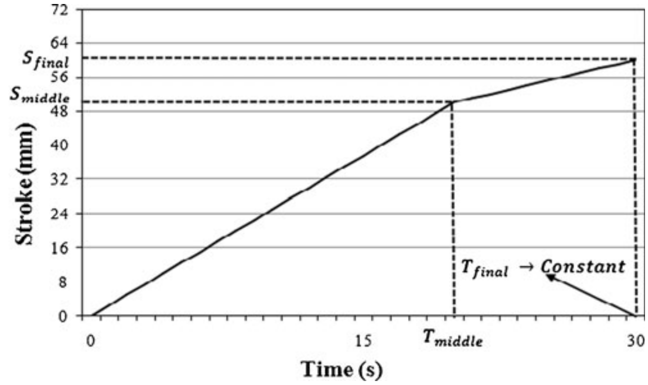

Fig. 3 The axial-punch path with three variables

distribution by applying different loading paths. Most of the studies done on determination of load paths in tube hydroforming are limited to investigating certain proposed paths and comparing their results to find the more effective ones in order to enhance some selected outputs. However, because of the interaction of different involved variables, finding the more appropriate load paths is still a complex task. Hence, to enhance the quality of hydroformed parts, more comprehensive studies are required.

The current study presents a new method for optimizing the loading parameters. Thirty-two different loading paths were designed using the design of experiments method. Then, the selected outputs including the minimum thickness and maximum height of protrusion of the tube were calculated by FE simulation when each load path was applied. The proposed model was implemented into a simulated annealing (SA) optimization procedure to identify the set of loading parameters that optimizes the outputs. To verify the optimum results, a comparison between the results of the SA algorithm and a genetic algorithm (GA) was performed.

2 Design of experiments

2.1 Tube hydroforming

Tube hydroforming is a process in which tubes are formed into a desired shape in a die by applying internal pressure. In this process, the capacity of the machine tool is directly related to the final pressure to be applied. However, in order to decrease thinning in the formed part, it is necessary to use axial feeding of the tube ends. Nowadays, a counterpunch is used to control the thickness distribution at the top of the protrusion in T-shaped or Y-shaped tubes. A schematic of T-shaped hydroforming is shown in Fig. 1. Because of the inherent complexity of the process and the existence of many effective parameters on the formability of the tube, the adjustment of all conditions is difficult; thus, designing an optimal set of all formation parameters is a major concern for manufacturers.

In the current study, the optimal loading conditions were determined for a fixed geometry and lubrication

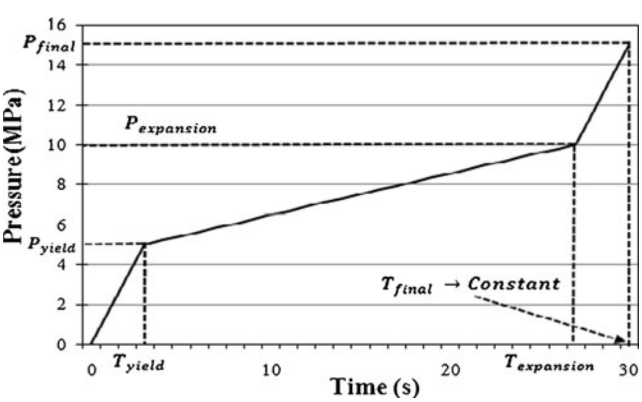

Fig. 2 The general path for internal pressure with the respective variables

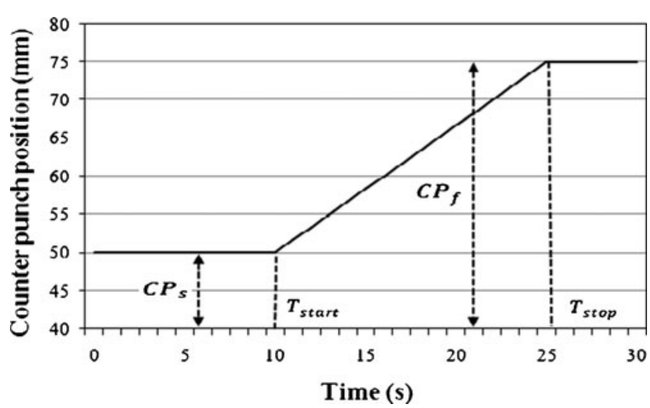

Fig. 4 The path of the counterpunch displacement with four variables

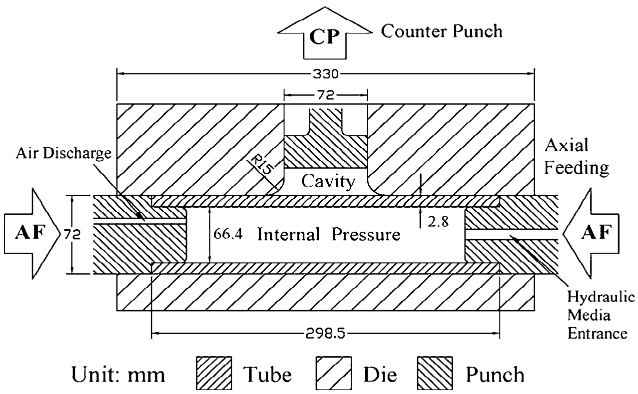

Fig. 5 Experimental model for T-shaped hydroforming [13]

condition. In order to optimize a general situation, a goal function which is usually an error function of outputs is needed. In the present study, the minimum thickness and maximum height of protrusion were chosen to prevent the occurrence of thinning and wrinkling. Hence, the goal function was built by these indexes. There were not an explicit analytical relation between forming indicators and loading variables; hence, the mathematical modeling applied in analysis of variance technique was utilized to construct the relation between the loading (input) variables and forming indicators (output variables). After determination of the loading variables, the lower and upper bounds for each variable were chosen. Then, different combinations of loading variables were obtained with the aid of Taguchi design. Each of these load paths were applied into the experimental model and the respective outputs were calculated to complete the Taguchi table. The regression analysis was used to create mathematical relations between the forming indexes and loading variables. These mathematical relations were used to build the goal function. The optimal values of loading variables were calculated by applying this function into the optimization algorithm. Then, according to these optimal values, the optimal load paths were generated. There are various optimization algorithms and two well-known algorithms contain simulated annealing and genetic algorithms used in this paper are discussed in the next parts.

2.2 Loading parameters

As described earlier, there are three main independent loading parameters in T-shaped tube hydroforming, including the internal pressure, axial-punch feeding, and counterpunch displacement.

(a) Internal pressure

Internal pressure is the most significant parameter in tube hydroforming. The main focus has been on choosing an appropriate pressure curve versus time in the tube hydroforming process. Cherouat et al. [6] investigated the effect of three different load curves for internal pressure and reported a successful forming using a pressure curve consisting of multiple stages. Hama et al. [7] obtained good formability for a hydroformed tube when he applied the pressure path designed according to three stages path. Some other researchers also used similar

Fig. 6 Half of the simulation model

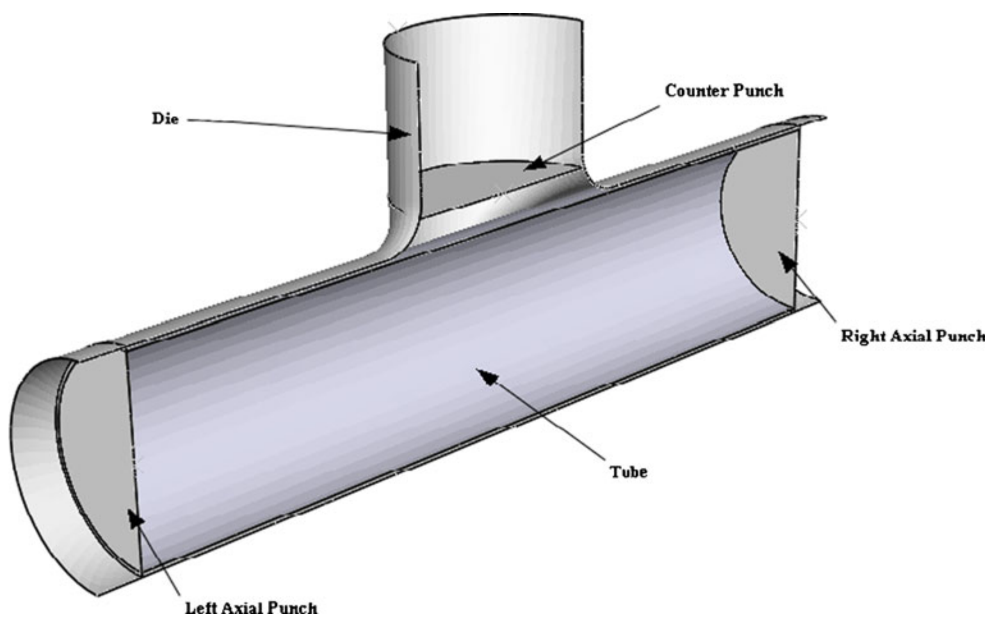

Table 1 Material properties of the tubular blank (AA6063-T5) [13]

Factor	Value
Young modulus E (GPa)	60
Poisson ratio υ	0.35
Yield stress σ_y (MPa)	55
Strength factor K (MPa)	181.09
Strain hardening exponent (n)	0.318
Anisotropy ($\overline{R}$)	0.5225

concepts to optimize the loading path of internal pressure.

If the total time of experiment can be taken as fixed, then five variables are sufficient to design the internal pressure curve, including the yielding (P_{yield}), expanding (P_{expan}) and calibration pressures (P_{final}) and their required times (T_{yield}) and (T_{expan}) as they are seen in Fig. 2. Yielding, expansion, and calibration pressure were evaluated in megapascals and their required time variables were evaluated in second (s). Although the yielding pressure (P_{yield}) was initially considered as a possible variable parameter in the analysis, a primary analysis of variance (ANOVA) proved that it can be fixed at 2.5 MPa, and this value was used in the rest of this analysis.

(b) Axial-punch feeding

The axial-punch displacement curves were similar in many reports and usually consist of two stages, such as in the studies done by Jirathearanat et al. [8], Imaninejad et al. [3], and Ray and Mac Donald [9]. Because of the symmetry, the left and right axial-punch feedings were similar and the loading path had only two variables for the displacement contain (S_{middle}) and (S_{final}) as the middle and final displacements, respectively. Moreover, (T_{middle}) is the time of the first variable (S_{middle}), see Fig. 3.

(c) Counter-punch displacement

The counterpunch was used to control the protrusion height and also to control the evolution of thickness and avoid over thinning. Boudeau et al. [10] used it for the T-shaped hydroforming process. Cheng et al. [11] investigated the hydroforming of a Y-shaped tube with an angle of 45° using FE simulation and experimentation. Generally, the path of the counterpunch displacement contains some variables, such as the starting time (in seconds) (T_{start}), amount of displacement in (millimeters) ($D_{\text{counterpunch}}$) and termination time (T_{stop}) in seconds. Two variables are usually used to determine the displacement of the counterpunch: its initial ($\mathrm{CP_s}$) and final position ($\mathrm{CP_f}$) in millimeters. The difference between these two variables shows the movement of the counterpunch $\left(D_{\text{counterpunch}} = \mathrm{CP_f} - \mathrm{CP_s}\right)$, as shown in Fig. 4. It should be noted that the position of the counterpunch was calculated from the centerline of the tube.

2.3 Indicators of tube formability in hydroforming

In T-shaped tube hydroforming, one objective is to manufacture the part with the maximum protrusion and minimum variation of tube wall thickness. On the other hand, these variables depend on the process parameters and are called the dependent or response variables in design of experiment. These two response parameters have been considered by many researchers to be the

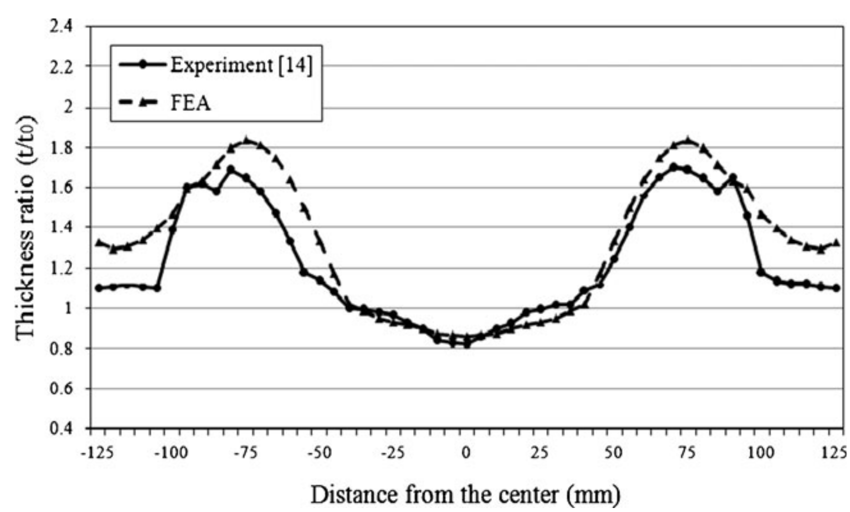

Fig. 7 Comparison of the thickness distribution of the centerline of the formed tube for the experimental and FEA models

Table 2 Comparison between the experimental results and the FE simulation

Indicator	Minimum thickness	Maximum height
Experiment (mm)	2.296	42
FE Simulation (mm)	2.401	41.3
Δ (percent, %)	4.57	1.67

objective functions in the optimization process [3, 5, 12]. It is worthy to note that usually, the minimum wall thickness and the height of protrusion are considered as the thinning and wrinkling indicators, respectively.

In the current study, the minimum thickness and maximum height of a T-branch were selected to assess and compare the application of different load paths. These two parameters were used to construct the objective or cost functions in the next sections of this study.

2.4 Experimental models

There are three main methods to design the experiments, i.e., the full factorial design, central composite design and Taguchi design. In the current study, the Taguchi method was used. Taguchi methods give us a good opportunity to develop new processes with the smallest number of experiments. The notation used for Taguchi methods has the form of $L_N(n^k)$. In this expression, L, N, n, and k are the symbols of the Taguchi methods, the total number of experiments, the number of levels for each variables and the number of existing variables in the experiment, respectively.

Table 3 Upper and lower bounds for the loading variables

Variable	Level	Value	Variable	Level	Value
P_{yield}	−	2.5	S_{final}	−	60
	+	6.5		+	64
P_{expan}	−	7.5	T_{middle}	−	20
	+	12.5		+	27
P_{final}	−	12.5	CP_s	−	50
	+	17.5		+	56
T_{yield}	−	2	CP_f	−	75
	+	4		+	81
T_{expan}	−	20	T_{start}	−	5
	+	27		+	10
S_{middle}	−	50	T_{stop}	−	20
	+	60		+	30

In the current process, k and n were selected as 11 and 2, respectively. The maximum number of experiments, N=32, was considered to cover most conditions. As a result, the L_{32} (2^{11}) method was used for this process.

2.5 Verification of the experimental model

The Abaqus/Explicit software was used to simulate T-shaped tube hydroforming process and to investigate the effects of different loading conditions. An experimental process carried out by Hwang [13] was used here to verify our computational procedure. The configuration of the die, tube, axial, and counterpunches is shown in Fig. 5, as it was used by Hwang. Half of the simulation model is shown in Fig. 6. A tube with a diameter of 72 mm was placed at the center of the T-shaped die with a wall thickness and length of 2.8 and 298.5 mm, respectively. Two axial-punches and one counterpunch were designed and assembled, as shown in Fig. 5. Aluminum alloy 6063-T5 tube was used in the experimental model. The mechanical properties of this material are listed in Table 1.

To consider the material anisotropy, Hill's model was assumed in the simulation. The tube was divided into three-dimensional shell elements (S4R), whereas the die and punches were modeled as rigid entities. The loading curves used in the simulation are specified in Ref. [13].

Using these specifications, the calculated thickness distribution for the centerline of the formed tube is shown in Fig. 7. This thickness was compared with the experimental results and there was a good agreement between them. The indicators were compared with the experimental ones and the calculation error was determined by $\Delta = |\text{Simulation} - \text{Exp}|/\text{Exp}$, Table 2. It can be seen that there is a small difference (error<5%) between the experimental and FEA results.

2.6 Determination of appropriate bounds for design variables

After verification the FEA model, suitable bounds for each variable were determined, which is an important issue in optimization of the design of experiment method. The variables were chosen according to the experimental models, FE simulations, analytical relations for the pressure and the nature of each variable. They are listed with their upper and lower bounds in Table 3.

Based on the Taguchi models shown in Table 4, three load paths were designed for each experiment and used to simulate the process. In total, 32 load paths were designed and four typical paths are illustrated in Fig. 8 for the internal pressure.

Table 4 Taguchi table and FE simulation results

Number	P_{expan}	P_{final}	T_{yield}	T_{expan}	S_{middle}	S_{final}	T_{middle}	CP_s	CP_f	T_{start}	T_{stop}	T (mm)	H (mm)
1	7.5	12.5	2	20	50	60	20	50	75	5	20	2.51	38.23
2	7.5	12.5	2	27	50	60	20	50	81	10	30	2.47	36.36
3	7.5	12.5	4	20	50	64	27	56	75	5	20	2.56	41.05
4	7.5	12.5	4	27	50	64	27	56	81	10	30	2.46	40.07
5	7.5	17.5	2	20	60	60	27	56	75	10	30	2.51	37.93
6	7.5	17.5	2	27	60	60	27	56	81	5	20	2.19	40.70
7	7.5	17.5	4	20	60	64	20	50	75	10	30	2.40	35.54
8	7.5	17.5	4	27	60	64	20	50	81	5	20	2.16	40.85
9	7.5	12.5	2	20	60	64	27	50	81	10	20	2.49	40.59
10	7.5	12.5	2	27	60	64	27	50	75	5	30	2.61	38.46
11	7.5	12.5	4	20	60	60	20	56	81	10	20	2.44	35.29
12	7.5	12.5	4	27	60	60	20	56	75	5	30	2.45	32.80
13	7.5	17.5	2	20	50	64	20	56	81	5	30	2.46	42.48
14	7.5	17.5	2	27	50	64	20	56	75	10	20	2.55	39.03
15	7.5	17.5	4	20	50	60	27	50	81	5	30	2.29	42.43
16	7.5	17.5	4	27	50	60	27	50	75	10	20	2.41	38.26
17	12.5	12.5	2	20	60	64	20	56	81	5	30	2.42	40.85
18	12.5	12.5	2	27	60	64	20	56	75	10	20	2.57	40.08
19	12.5	12.5	4	20	60	60	27	50	81	5	30	2.26	40.48
20	12.5	12.5	4	27	60	60	27	50	75	10	20	2.52	38.47
21	12.5	17.5	2	20	50	64	27	50	81	10	20	2.28	46.29
22	12.5	17.5	2	27	50	64	27	50	75	5	30	2.49	42.04
23	12.5	17.5	4	20	50	60	20	56	81	10	20	2.30	42.43
24	12.5	17.5	4	27	50	60	20	56	75	5	30	2.45	37.98
25	12.5	12.5	2	20	50	60	27	56	75	10	30	2.58	40.85
26	12.5	12.5	2	27	50	60	27	56	81	5	20	2.44	42.57
27	12.5	12.5	4	20	50	64	20	50	75	10	30	2.59	38.94
28	12.5	12.5	4	27	50	64	20	50	81	5	20	2.44	41.20
29	12.5	17.5	2	20	60	60	20	50	75	5	20	2.40	38.86
30	12.5	17.5	2	27	60	60	20	50	81	10	30	2.22	35.49
31	12.5	17.5	4	20	60	64	27	56	75	5	20	2.41	42.15
32	12.5	17.5	4	27	60	64	27	56	81	10	30	2.35	42.34

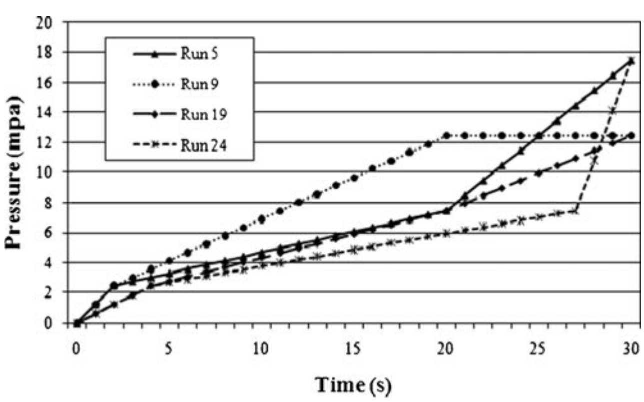

Fig. 8 Four sample paths for the internal pressure

2.7 FEA of the Taguchi design

Each set of load paths were applied into the FE model and the results obtained from the simulation for two indicators of formability, including the minimum thickness and maximum height of the protrusion, were obtained and listed in the last two columns of Table 4.

3 Analysis of variance

3.1 Regression analysis

In this study, analysis of variance (ANOVA) was used to investigate each variable and to estimate the tube

Table 5 ANOVA for minimum thickness according to linear model

Source	DF	Seq SS	Adj SS	Adj MS	*F* value	*T* value	*P* value
P_{expan}	1	0.001800	0.001800	0.001800	0.61	−0.78	0.443
P_{final}	1	0.117612	0.117613	0.117613	40.01	−6.33	0.000
T_{yield}	1	0.015313	0.015313	0.015313	5.21	−2.28	0.034
T_{expan}	1	0.000450	0.000450	0.000450	0.15	−0.39	0.700
S_{middle}	1	0.024200	0.024200	0.024200	8.23	−2.87	0.009
S_{final}	1	0.020000	0.020000	0.020000	6.80	2.61	0.017
T_{middle}	1	0.000013	0.000013	0.000013	0.00	0.07	0.949
CP_s	1	0.011250	0.011250	0.011250	3.83	1.96	0.065
CP_f	1	0.171113	0.171113	0.171113	58.21	−7.63	0.000
T_{start}	1	0.011250	0.011250	0.011250	3.83	1.96	0.065
T_{stop}	1	0.003613	0.003613	0.003613	1.23	1.11	0.281
Error	20	0.058787	0.058787	0.002939			
Total	31	0.435400					
R square=86.7%				*R* adjusted=79.1%			

formability. The first step in ANOVA was the creation of a proper model between dependent variables (thickness and height) and other independent variables (loading parameters), which was carried out by regression analysis.

Building upon the results of the proposed models, the table of design of experiment was carried out by regression analysis. Each output variable was fitted by linear, exponential, and stepwise models. The curvilinear model cannot estimate the tube formability accurately without information from a large number of experiments. The regression analysis in this study was investigated with the MINITAB software.

$$\begin{aligned} \text{Thickness} = {} & 3.89 - 0.00341\, P_{expan} - 0.0244\, P_{final} \\ & - 0.0219 T_{yield} - 0.00087\, T_{expan} \\ & - 0.00544\, S_{middle} + 0.0122\, S_{final} \\ & + 0.00019\, T_{middle} + 0.00671\, CP_s \\ & - 0.0244\, CP_f + 0.00742\, T_{start} \\ & + 0.00213\, T_{stop}. \end{aligned} \tag{1}$$

Table 6 ANOVA for protrusion height according to linear model

Source	*df*	Seq SS	Adj SS	Adj MS	*F* value	*T* value	*P* value
P_{expan}	1	29.934	29.934	29.934	27.49	5.24	0.000
P_{final}	1	10.707	10.707	10.707	9.83	3.14	0.005
T_{yield}	1	3.465	3.465	3.465	3.18	−1.78	0.090
T_{expan}	1	9.779	9.779	9.779	8.98	−3.00	0.007
S_{middle}	1	26.883	26.883	26.883	24.69	−4.97	0.000
S_{final}	1	33.682	33.682	33.682	30.93	5.56	0.000
T_{middle}	1	45.769	45.769	45.769	42.03	6.48	0.000
CP_s	1	1.167	1.167	1.167	1.07	1.04	0.313
CP_f	1	27.658	27.658	27.658	25.40	5.04	0.000
T_{start}	1	7.192	7.192	7.192	6.60	−2.57	0.018
T_{stop}	1	13.794	13.794	13.794	12.67	−3.56	0.002
Error	20	21.776	21.776	1.089			
Total	31	231.806					
R square=90.60%				*R* adjusted=85.4%			

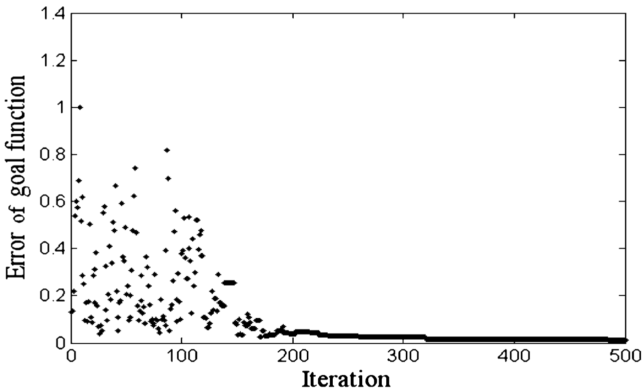

Fig. 9 Convergence of the SA algorithm

$$\begin{aligned}\text{Height} = &-15.5 + 0.387\,P_{\text{expan}} + 0.231\,P_{\text{final}} \\ &- 0.329\,T_{\text{yield}} - 0.158\,T_{\text{expan}} - 0.183\,S_{\text{middle}} \\ &+ 0.513\,S_{\text{final}} + 0.342\,T_{\text{middle}} + 0.0636\,\text{CP}_{\text{s}} \\ &+ 0.310\,\text{CP}_{\text{f}} - 0.190\,T_{\text{start}} - 0.131\,T_{\text{stop}}. \qquad (2)\end{aligned}$$

3.2 ANOVA

The adequacies of the above models were evaluated by ANOVA technique [14]. An effective criterion for the adequacy of a model is the correlation factor, i.e., correlation factors approaching 100% indicate high accuracy. The correlation factors for the different regression models are tabulated in the last rows of Tables 5 and 6. Based on the correlation factors and P value, the linear model provides a better representation of the actual process in terms of the thickness and height response and can be used in the optimization design.

The main usage of ANOVA is investigating the effect of input (loading variables) on output variables (tube formability indicators) to remove the non-significant input variables. It was achieved by calculating the F values for both input and output variables, Tables 5 and 6. It is seen that the five variables (T_{yield}, T_{expan}, T_{start}, CP_{s}, and T_{stop}) do not have any significant effect on the outputs and can be fixed in the process. Hence, the mathematical models were embedded to the optimization algorithms initially. Then, after calculation of optimum values, a new design based on the six remaining variables were investigated. Therefore, these five variables were removed from design of experiment and were considered as constant parameters such as geometrical parameters in FE model.

3.3 Optimization

Two well-known methods, i.e., the SA algorithm and the GA, were used here to seek the optimum values for each variable.

3.3.1 Simulated annealing algorithm

The SA algorithm was first proposed by Metrols [15]. Later, Kirkpatrick [16] developed it further and used it as a powerful optimization method. The SA algorithm was originally inspired by analogous physical process of heating, when slowly cooling to reach a stable crystalline structure. There are striking similarities between annealing and optimization processes based on the search for minimum value for a function. In the annealing process, this function is the total energy of structure, which needs to be minimized in such a way that every particle can settle in a proper place. In an optimization process, a cost function should be minimized. The algorithm starts by generating a random initial solution. Then, a new solution in the neighborhood of the current solution is constructed by making a small random change. The value of the objective function for the former random solution is compared with that of the later solution.

Table 7 The obtained optimum values for the design of load paths

Number	Optimum variables obtained by SA									
	P_{expan}	P_{final}	T_{yield}	T_{expan}	S_{middle}	S_{final}	T_{middle}	CP_{s}	CP_{f}	T_{start}	T_{stop}
1	10.5	13.5	2	20.5	50	63.5	27	56	75	7	30
2	11	12.5	2	21	52	64	23	56	75	10	28
3	9.5	12.5	2	24.5	50	63.5	25.5	56	75.5	9.5	30
4	12	12.5	2.4	22.5	52	64	26.5	53.5	76.5	6.5	30
5	7.5	12.5	2	21.5	50	64	26.5	56	75	10	30

Table 8 The final results of the SA algorithm and the FEA for the optimum load path

SA		Abaqus	
T (mm)	H (mm)	T (mm)	H (mm)
2.66	39.91	2.55	40.8

3.3.2 Optimizing the loading parameters by the SA algorithm

A proper function needs to be defined for this process in such a way that it involves all loading variables and the index of formability. An appropriate function for this purpose can be the error function, which is based on two indicators of formability and has the following form;

$$f = \frac{(T_{\exp} - T)^2}{T_{\exp}} + \frac{(H_{\exp} - H)^2}{H_{\exp}}. \qquad (3)$$

This function is equal to the total energy in a structure and should be minimized. In the above function, $T_{\exp}$ and $H_{\exp}$ were calculated by Eqs. 1 and 2, respectively; T and H were the desired values chosen by the designer. Here, T was equal to initial thickness of the tube, or 2.8 mm, and H was equal to total axial-punch displacement. As seen in Table 4, the best value for this parameter is 46.29 mm; however, to reduce the error of the goal function, that value was considered to be 50 mm.

The proposed SA algorithm was programmed in the MATLAB software. The convergence curve for one sample is shown in Fig. 9. This curve illustrates that the algorithm converges rapidly and the desire input variables are obtained before 300 iterations. Five sets of optimum input variables determined by SA code are tabulated in Table 7. For each set of load path obtained by SA algorithm, a FEA simulation was carried out and the accuracy of the algorithm was proved. Based on the minimum difference between the SA results and FE simulations, the third set was chosen for design of optimal path. The outputs according to these optimal paths are summarized in Table 8. It can be seen that the SA algorithm is accurate enough.

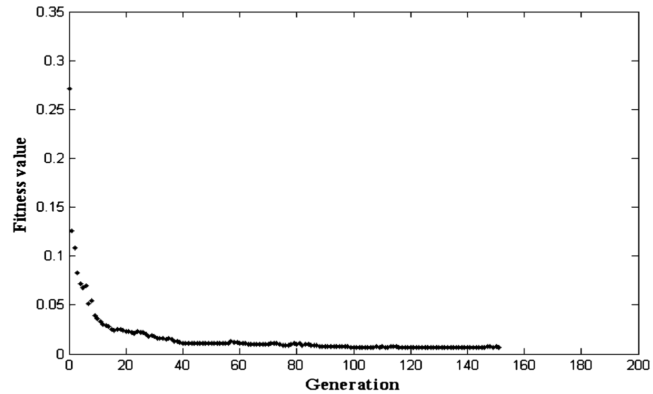

Fig. 10 Convergence of the GA

3.3.3 Optimization of the loading parameters by the genetic algorithm

The GA is a search algorithm that works according to the natural selection inspired from the theory of natural evolution [17]. The GA is a robust method to search for the optimum solution and is used in a wide range of problems. In general, the GA proposed a solution using strings (usually referred to as chromosomes) of variables that construct the problem [18].

In this study, the objective function was Eq. 3, and all input variables with their respective bounds were as they have already described. After giving an objective function, the input variables with their bounds, the crossover rate, the mutation rate, the population size, and the number of iteration were determined. Then, an initial population based on random selection was generated. After that, the first input variables were coded in some string structures. Binary-coded strings having 0's and 1's were usually used. When the coding of input variables was completed, an appropriate value for X_i was found. By substituting the input variables in the objective function, the function value was calculated. The fitness function value of a string is known as the string fitness.

The operation of the GA begins with a population of a random string representing design or decision variables. The population was then operated on by three main operators, reproduction, crossover, and mutation to create a new population of points. Applying these operators to the current population created a new population. This new

Table 9 The optimum values of load paths calculated from the GA

P_{expan}	P_{final}	T_{yield}	T_{expan}	S_{middle}	S_{final}	T_{middle}	$\mathrm{CP_s}$	$\mathrm{CP_f}$	T_{start}	T_{stop}
10.501	12.543	2.013	20.839	50.352	63.93	26.976	55.904	75.998	9.445	27.773

Table 10 The selected loading variables with new bounds

Number	Factor	Unit	Lower bounds (−)	Upper bound (+)
1	P_{expan}	Mpa	7.5	11
2	P_{final}	Mpa	12	14
3	S_{middle}	mm	50	56
4	S_{final}	mm	61	65
5	T_{middle}	s	23	27
6	CP_f	mm	74	80

population was used to generate subsequent populations and so on. The values of the objective function of the individuals of the new population were determined again by decoding the strings. Each completed cycle of the GA is called a new generation. In each generation, if the solution was improved, that solution was stored as the best solution. This process continued until convergence.

The GA was programmed in Matlab software and according to the mentioned objective function, the optimum values for each design variables were calculated as they are listed in Table 9. The convergence rate is seen in Fig. 10. A comparison between the obtained results and the ones from the SA algorithm (Tables 7 and 9) shows a good accuracy and agreement between them. It has to be noted that the five loading variables contain T_{yield}, T_{expan}, CP_s, $T_{start,}$ and T_{stop} were fixed in the simulation according to the best values of third set in Table 7.

4 Full factorial design

There are six remaining variables that can be considered to cover all conditions of loading parameters, and the full factorial method was used to design their corresponding load paths. At first, the respective bounds for each variable must be modified according to optimum results, see Table 10. Based on the two-level experiments, 64 load paths were designed with the MINITAB software. Since, the full factorial design is a well-known method for researchers, therefore the respective design and FEA results are not reported in this study, and only the results obtained from ANOVA are investigated in following.

Table 11 ANOVA results for curvilinear model of tube formability

Parameter	Thickness	Height
R square, %	92.3	88.5
R adjusted, %	98.9	98.4
F value	23.98	187.01
P value	0.000	0.000

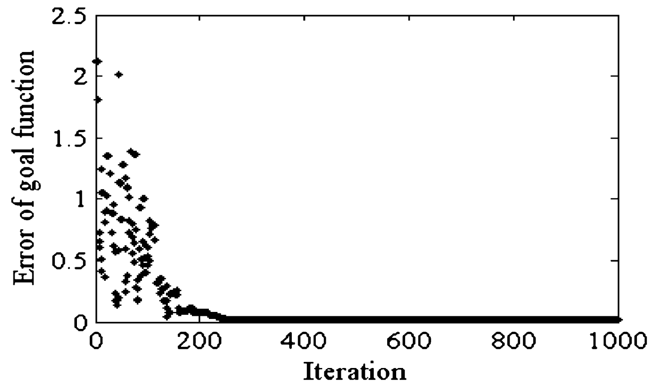

Fig. 11 Convergence curve of the SA algorithm for this problem

4.1 ANOVA based on full factorial design

Although it is possible to enhance the formability of the tube by using a higher degree model, it was found that using a curvilinear model to calculate the two outputs of this study lead to better accuracy.

Curvilinear models:

$$\begin{aligned}\text{Thickness} = {} & 11.6 - 0.191P_{expan} + 0.0555P_{final} \\ & - 0.0357S_{middle} - 0.123S_{final} - 0.0412T_{middle} \\ & - 0.0727CP_f + 0.00237P_{expan}P_{final} \\ & + 0.000074P_{expan}S_{middle} - 0.000469P_{expan}S_{final} \\ & - 0.000558P_{expan}T_{middle} + 0.00251P_{expan}CP_f \\ & + 0.000026P_{final}S_{middle} + 0.00184P_{final}S_{final} \\ & - 0.00020P_{final}T_{middle} - - 0.00258P_{final}CP_f \\ & + 0.000820S_{middle}S_{final} + 0.00118S_{middle}T_{middle} \\ & - 0.000582S_{middle}CP_f - 0.00131S_{final}T_{middle} \\ & + 0.00129S_{fina}lCP_f + 0.000820T_{middle}CP_f\end{aligned} \tag{4}$$

$$\begin{aligned}\text{Height} = {} & 195 - 1.91P_{expan} - 1.72P_{final} \\ & - 0.740S_{middle} - 1.66S_{final} - 0.886T_{middle} \\ & - 2.18CP_f - 0.0421P_{expan}P_{final} \\ & + 0.00298P_{expan}S_{middle} - 0.0142P_{expan}S_{final} \\ & + 0.00920P_{expan}T_{middle} + 0.0442P_{expan}CPf \\ & + 0.0056P_{final}S_{middle} - 0.0086P_{final}S_{final} \\ & + 0.0170P_{final}T_{middle} + 0.0268P_{final}CP_f \\ & + 0.0102S_{middle}S_{final} + 0.00245S_{middle}T_{middle} \\ & - 0.00288S_{middle}CP_f - 0.00547S_{final}T_{middle} \\ & + 0.0257S_{final}CP_f + 0.0141T_{middle}CP_f\end{aligned} \tag{5}$$

To study the adequacy of above model, the respective values for (*R*-Sq), (*R*-Sq(adj)), (*P* value), and (*F* value) were calculated in order to determine the adequacy of the

Table 12 The optimum set of loading variables for the design of load paths

P_{expan}	P_{final}	T_{yield}	T_{expan}	S_{middle}	S_{final}	T_{middle}	CP_s	CP_f	T_{start}	T_{stop}
9.7	12	2	24.5	50	65	23	56	78	9.5	30

above model. These values are shown in Table 11 and they indicate that the model is very accurate. Then, the SA algorithm was made according to curvilinear model and the optimal load curves were achieved.

4.2 Optimization versus the full factorial design

The proposed SA algorithm was used to determine the optimal values of the input variables. The optimization process was carried out based on the curvilinear model. The objective function (Eq. 3) was used again and the aforementioned models were inserted in this function. The T_{exp} and H_{exp} were calculated by Eqs. 4 and 5, respectively. The T and H are the desired values and are selected by the designer, as discussed in Section 3.3.2.

The proposed SA code was written in the Matlab programming software, and the convergence of this algorithm is shown in Fig. 11. Five sets of input variables were calculated and the results of each set of the SA algorithm and FE simulation and their respective errors were determined. Based on the FE simulation and minimum obtained error, the final input variables were found to be used in designing of load paths, Table 12. The corresponding outputs are shown in Table 13 and the optimal load paths are shown in Figs. 12, 13, and 14 for internal pressure and axial and counterpunches, respectively. The general shape of tubular part formed by applying these load paths is similar to that shown in Fig. 15. However, by comparing Tables 8 and 13 it can be found that the specifications of tube formability are improved significantly.

In comparing the two methods of optimization used in the Taguchi and full factorial method, it was found that the SA algorithm converged to optimal results rapidly for both linear and curvilinear models. However, the full factorial design consumed more CPU time in FE analysis for nonlinear models compared with the linear ones. But, using a high speed computer and utilizing the mass scaling concept in Abaqus/Explicit could decrease the total CPU time. The better models always reduce experimental costs by eliminating expensive trial-and-error experimental methods in laboratory.

Table 13 Desired outputs based on the optimum load path

SA		Abaqus	
T (mm)	H (mm)	T (mm)	H (mm)
2.59	42.18	2.55	42.23

5 Discussion

The aim of this study was to show that it is possible to find the optimal set of hydroforming process parameters without having an explicit relation between the inputs and the outputs. In fact, the method does not depend on how complicated the problem is and how many effective parameters are in the process. Another capability of the proposed method is that during the experimental process, one can realize the non-optimized values. Moreover, it is possible to determine the optimized values even with arbitrary initial values. For instance, the analysis of variance showed that the yielding pressure for a material with prescribed conditions was a specified value. Furthermore, it is possible to study the effect of each input on the output variables (the minimum thickness and maximum height) based on the analysis of variance. Meanwhile, inaccurate ranges can be modified to find more appropriate ranges containing the optimums.

It can be observed from Figs. 9, 10, and 11 that in both algorithms, the optimal results were determined with a high convergence rate. The optimal results for the loading variables were calculated in less than 200 iterations. However, the comparison revealed that the SA algorithm was more effective than the GA. In the SA algorithm, the proper intervals are defined for the values. Moreover, a special step is required for each variable which helps the designer to determine the optimal value for a variable.

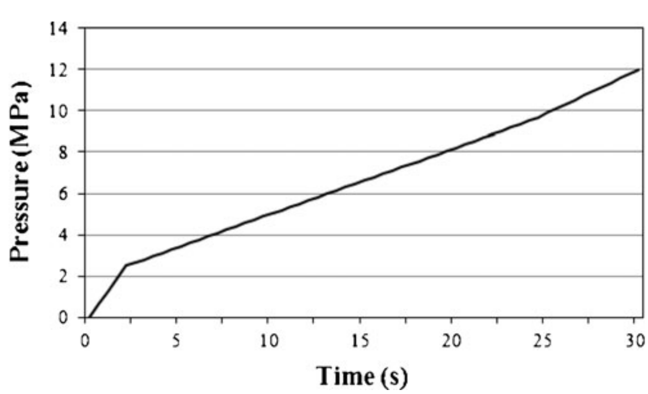

Fig. 12 The optimum path for the internal pressure

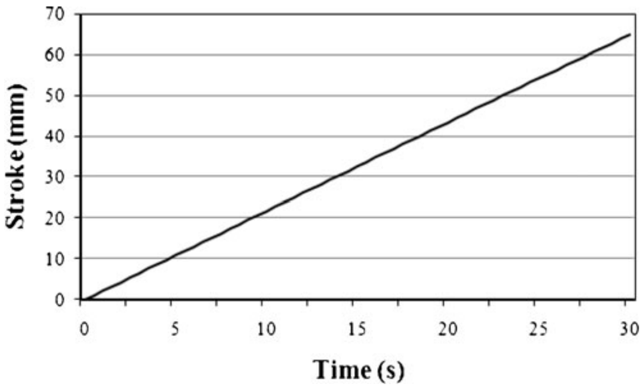

Fig. 13 The optimum axial-punch obtained from the SA algorithm

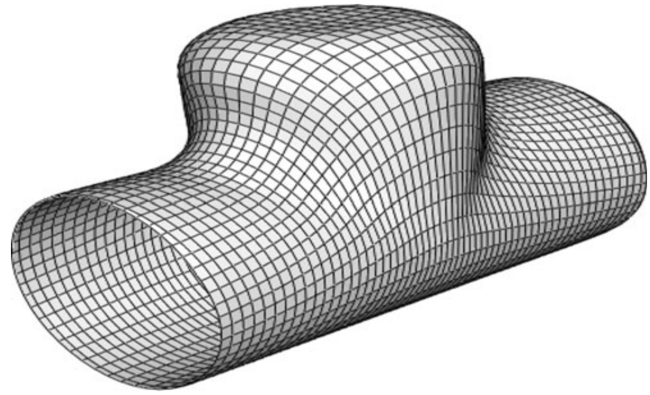

Fig. 15 The formed tube under optimal loading conditions

However, the GA finds the optimum value over the whole domain. Furthermore, the optimum value is only a real value and it may not be a reasonable value for the experimental purpose. For example, in the current study, for the variable CP_s the value of 55.904 was calculated which was not applicable in the experimental. Hence, the GA was used only for the control of accuracy of optimal results of SA algorithm.

To investigate the effectiveness of the proposed method in the design of the optimal load path, the results obtained from this method were compared with the experimental results of Hwang [13]. The following remarks may be emphasized in this comparison.

- The main parameter in the design of load paths is the internal pressure curve and the final pressure, which determines the capacity of the press instrument. In fact, decreasing the pressure capacity by only 1% has a significant influence on the price of the products.
- An important parameter in the quality of products is the thinning of the formed tube. The experimental model of Hwang is used here to assess the current obtained results.
- The height of the protrusion is another important parameter and has a reverse relation with the thinning value.

The optimal results of the current study with experimental results of Hwang [13] are displayed in Table 14. The thinning value was calculated as follows;

$$\text{Thinning} = 100 \times \left(\frac{T_{\text{initial}} - T_{\text{final}}}{T_{\text{initial}}} \right) \qquad (6)$$

where T_{final} was the minimum thickness of tube at the end of forming, and T_{initial} was the initial thickness of tube, which was equal to 2.8 mm. In the hydroforming process, the thinning was allowed to be ±15%, and in the Hwang study it was considered to be ±20%.

It was observed that the final pressure in our study was 20% less than that in Hwang experiment, and the thinning value for the tube in the verified model of the Hwang experiment was decreased from 14.3% to 8.8% for the optimum current calculation. At the same time, the protrusion height of the branch did not decrease; in fact, it increased a small amount. In general, the proposed method was established based on all variables and the optimal results are reliable.

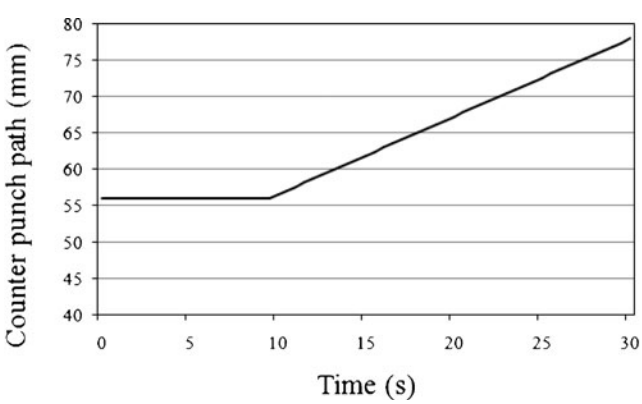

Fig. 14 The optimum counterpunch displacement calculated by the SA algorithm

6 Conclusion

In this paper, a new method was established to optimize the loading variables in the hydroforming process. First, through a statistical analysis in conjunction with FE

Table 14 The comparison of results

Results	Factor	Hwang	FEA of Hwang	Optimum
Final pressure	(MPa)	15	15	12
Thinning	(%)	18	14.3	8.8
Protrusion height	(mm)	42	41.3	42.23

analysis, the mathematical relation between the input and output variables was calculated and the influence of loading variables on the forming indicators was studied. Then, by inserting the mathematical models into an evolutionary algorithm, the optimal load paths for this process were achieved. The comparison of the obtained results with the experimental results verified the efficiency of this method. The proposed method could be used in processes with no specific relations between the inputs and outputs. In addition, by finding the mathematical relations and by exploring the effects of inputs on the outputs, the optimal conditions for experiments could be determined. The method proposed here may be applied to many hydroformed parts such as T, Y, and X-shaped tubular components. Moreover, even for parts that do not have a protrusion, this method will help to minimize the maximum forming pressure. Finally, minimizing the thickness variation is another objective required by the designers.

Nomenclatures

CP_s	Initial position of counterpunch
CP_f	Final position of counterpunch
$D_{counterpunch}$	Movement of counterpunch
E	Young modulus
H	Height of protrusion
K	Strength factor
k	Number of existing variables in the experiment
L	Symbol of the Taguchi method
N	Total number of experiments
n	Number of levels for each variables
P_{expan}	Expanding pressure
P_{final}	Calibration pressure
P_{yield}	Yielding pressure
S_{final}	Final displacement of axial-punch
S_{middle}	Middle displacement of axial-punch
T	Thickness of tube
T_{expan}	Expanding time
T_{middle}	Middle displacement time of axial-punch
T_{start}	Starting time of counterpunch
T_{stop}	Termination time of counterpunch
T_{yield}	Yielding time
S_{final}	Final displacement of axial-punch
S_{middle}	Middle displacement of axial-punch
υ	Poisson ratio
σ_y	Yield stress

References

1. Bardelcik A, Worswick MJ (2008) The effect of end-feed on straight and pre-bent tubular hydroforming of DP600 tubes, NUMISHEET 2008, September 1–5, Interlaken, Switzerland, 651–656
2. Rimkus W, Bauer H, Mihsein MJA (2000) Design of load-curves for hydroforming applications. J Mater Process Technol 108:97–105
3. Imaninejad M, Subhash G, Loukus A (2005) Loading path optimization of tube hydroforming process. Int J Mach Tools Manuf 45:1504–1514
4. Koç M, Altan T (2002) Application of two dimensional (2D) FEA for the tube hydroforming process. Int J Mach Tools Manuf 42:1285–1295
5. Lang L, Yuan S, Wang X, Wang ZR, Fu Z, Danckert J, Nielsen KBA (2004) Study on numerical simulation of hydroforming of aluminum alloy tube. J Mater Process Technol 146:377–388
6. Cherouat A, Saanouni K, Hammi Y (2002) Numerical improvement of thin tubes hydroforming with respect to ductile damage. Int J Mech Sci 44:2427–2446
7. Hama T, Ohkubo T, Kurisu K, Fujimoto H, Takuda H (2006) Formability of tube hydroforming under various loading paths. J Mater Process Technol 177:676–679
8. Jirathearanat S, Hartl C, Altan T (2004) Hydroforming of Y-shapes-product and process design using FEA simulation and experiments. J Mater Process Technol 146:124–129
9. Ray P, Mac Donald BJ (2004) Determination of the optimal load path for tube hydroforming processes using a fuzzy load control algorithm and finite element analysis. Finite Elem Anal Des 41:173–192
10. Boudeau N, Lejeune A, Gelin JC (2002) Influence of material and process parameters on the development of necking and bursting in flange and tube hydroforming. J Mater Process Technol 125–126:849–855
11. Cheng DM, Teng BG, Guo B, Yuan SJ (2009) Thickness distribution of a hydroformed Y-shape tube. Mater Sci Eng A 499:36–39
12. Lin FC, Kwan CT (2004) Application of abductive network and FEM to predict an acceptable product on T-shape tube hydroforming process. Comput Struct 15–16:1189–1200
13. Hwang YM, Lin TC, Chang WC (2007) Experiments on T-shape hydroforming with counter punch. J Mater Process Technol 192–193:243–248
14. Douglas CM (1996) Introduction to linear regression analysis, 2nd edn. Wiley, New York, pp 8–15
15. Catoni O (1996) Metropolis, Simulated annealing and iterated energy transformation algorithms: theory and experiments. J Complex 12:595–623
16. Teodorovic D, Pavkovic G (1992) A simulated annealing technique approach to the vehicle routing problem in the case of stochastic demand. Transport Plan Technol 16:261–273
17. Holland J (1975) Adaptation in natural and artificial systems. University of Michigan Press, Ann Arbor
18. Kaya IA (2009) Genetic algorithm approach to determine the sample size for attribute control charts. Inf Sci 179:1552–1566
19. Koç M, Altan T (2001) An overall review of the tube hydroforming (THF) technology. J Mater Process Technol 108:384–393